Optimal development of matrix elasticity

Stephanie Majkut[1,2], **Timon Idema**[2,4], **Joe Swift**[1], **Christine Krieger**[1], **Andrea Liu**[2], and **Dennis E. Discher**[1,2,3,*]

[1]Molecular and Cell Biophysics Lab, University of Pennsylvania, Philadelphia, PA 19104, USA
[2]Department of Physics and Astronomy, University of Pennsylvania, Philadelphia, PA 19104, USA [3]Cell and Molecular Biology Graduate Group, University of Pennsylvania, Philadelphia, PA 19104, USA [4]Department of Bionanoscience, Kavli Institute of Nanoscience, Delft University of Technology, Lorentzweg 1, 2628 CJ Delft, The Netherlands

Summary

In development and differentiation, morphological changes often accompany mechanical changes [1], but it is unclear if or when cells in embryos sense tissue elasticity. The earliest embryo is uniformly pliable while adult tissues vary widely in mechanics from soft brain and stiff heart to rigid bone [2], but the sensitivity of cells to microenvironment elasticity is debated [3]. Regenerative cardiology provides strong motivation because rigid post-infarct regions limit pumping by the adult heart [4]. Here we focus on embryonic heart and isolated cardiomyocytes, which both beat spontaneously. Tissue elasticity, E_t, increases daily for heart to 1-2 kiloPascal by embryonic day-4 (E4), and although this is ∼10-fold softer than adult heart, the beating contractions of E4-cardiomyocytes prove optimal at ∼$E_{t,E4}$ both *in vivo* and *in vitro*. Proteomics reveals daily increases in a small subset of proteins, namely collagen plus cardiac-specific excitation-contraction proteins. Rapid softening of the heart's matrix with collagenase or stiffening it with enzymatic crosslinking suppresses beating. Sparsely cultured E4-cardiomyocytes on collagen-coated gels likewise show maximal contraction on matrices with native E4 stiffness, highlighting *cell-intrinsic* mechanosensitivity. While an optimal elasticity for striation proves consistent with the mathematics of force-driven sarcomere registration, contraction wave-speed is linear in E_t as theorized for Excitation-Contraction Coupled to Matrix Elasticity. Mechanosensitive stem cell cardiogenesis helps generalize tissue results, which demonstrate how myosin-II organization and contractile function is optimally matched to the load presented by matrix elasticity.

Keywords

Mechanobiology; Heart; Development; Collagen; Cytoskeleton

*Correspondence: University of Pennsylvania, 129 Towne Bldg, Philadelphia, PA 19104-6393, discher@seas.upenn.edu, ph: 215 - 898 - 4809, fax: 215 - 573 – 2093.

Results and Discussion

The heart is the first functional organ in vertebrate embryos. Its beats spontaneously as a heart tube by ~36 hr after fertilization (Fig. 1A). Subsequent stiffening has been described thusfar in terms of changes in cell volume, hyaluronic acid, and/or collagen-I [5] – but functional tests are lacking. Cardiomyocytes isolated from either late embryos [6, 7] or neonates [8, 9, 10] and cultured on substrates of varied stiffness suggest that gels which are stiffer than adult heart suppress contraction. Extremely soft substrates suppress sarcomere organization and limit contractile ability, with additional evidence of altered cytoskeletal conformation and assembly [6] in the absence of changes evident in other cells such as mechanosensitive degradation [11] or transcription [12]. Mature cells cultured on gels can thus exhibit an optimal stiffness for contraction, but relevance of matrix elasticity to intact heart remains unclear and controversial based on handful of culture studies (eg. [3]).

Heart stiffens with expression of Excitation/Contraction/Collagen proteins, while Brain remains soft

Tissue aspiration into micropipettes (Fig. 1B) of diameter sufficient to probe dozens of cells [1] shows that heart at all stages behaves elastically (Fig. 1C) whereas midbrain tissue and embryonic disk flow over minutes and fail to recover fully after release of the stress. The effective Young's modulus of each tissue, E_t, was calculated from the slope of aspiration pressure versus aspirated length (Fig. S1A) [13], and for brain and embryonic disc, the (already large) aspirated length at 2 min was used. By E2, the presumptive ventricle is already 3-fold stiffer than undifferentiated embryonic disc and embryonic brain. The latter remains roughly constant through development at 0.3 ±0.2 kPa (Fig. 1D) and matches adult brain stiffness [14]. Brain tissue is thus always soft whereas heart stiffens up to about 10-fold to reach neonate and adult heart stiffness by E14 [6]. Modest stiffness variations of ±20% along the heart tube (Fig. S1B) are also consistent with past reports [15].

Expression trends for at least some tissue proteins seemed likely to parallel the trends in tissue mechanics and to confer tissue stiffness. Quantitative mass spectrometry of extracts from embryonic discs, and E2-E4, and E10 heart and brain tissue identified over 200 diverse proteins (Table S1), of which fewer than 10% followed trends in expression similar to those of E_t (Fig. 1D-H, S1C-D). Most trend-following proteins related closely to the excitation-contraction coupling system such as cardiac actomyosin contractile proteins, adhesion proteins, and the SERCA channel. Mitochondrial proteins (relevant to energetics) also followed the trends but at lower abundance. Proteins that were notably not correlated with tissue stiffness included many nuclear proteins, intermediate filament proteins, and nonmuscle myosin. Of two ECM proteins detected, only collagen-I follows the E_t trends.

To begin to assess stiffness contributions of the actomyosin cytoskeleton or collagen, we inhibited myosin contractility with the myosin-II ATPase inhibitor blebbistatin or else disrupted the collagenous ECM with mild collagenase treatments, and then measured tissue stiffness. With blebbistatin, heart tissue from E2 to E14 is softened by ~25% and brain tissue by ~50% (Fig. S1E). In contrast, collagenase had no significant effect on brain tissue but considerably softened both early and late heart (Fig. S1F) – without perturbing myosin-

II levels (Fig. S1G). The stiffness of brain tissue thus seems cellular in nature, whereas heart tissue mechanics have major extracellular matrix contributions at even the earliest functional stage of beating.

Optimal elasticity of embryonic heart: modest softening or stiffening impairs beating at E4

Embryonic heart tubes beat spontaneously at ∼1 Hz for up to 1-2 days after isolation, and we could easily measure local tissue strain in heart tubes during beating by imaging GFP transfected cells as fiducial markers (Fig. 2A). This very visible activity is used to address the main question of our studies: whether cells in an intact living tissue are sensitive to microenvironment elasticity. Controlled dose-time treatments with collagenase provided a simple means of softening tissue matrix (in just 30 min), while enzymatic crosslinking of ECM with transglutaminase provided a similarly rapid method to stiffen tissue (Fig. S2A,B). Enzyme permeated the tissue (Fig. S2C), and for all but the most extreme softening treatment, embryonic heart behaved elastically in micropipette aspiration (Fig. S2B-inset). By transfecting cells with a GFP membrane protein (SIRPA-GFP) we could also see that the contours of beating cells were unaffected by collagenase (Fig. 2B, S2D). Tissue softening is thus due primarily to cleavage of ECM rather than disruption of cell connections.

After the enzymatic treatments, hearts continue to beat rhythmically (Movies S1), but the magnitude of local contraction (calculated from GFP expressing cells) was always affected. Each heart tube region was analyzed separately (Fig.S2E-I), and normalization to pre-treatment measurements accounted for slight variations (∼20%) in embryo age and/or lab temperature. Untreated tissue invariably showed the largest contraction, which was typically ∼10% strain, while both softening and stiffening of the heart suppressed contractile strain (Fig. 2C, S2E). Stiffening of tissue should suppress strain since any muscle cell has a finite capacity to work against a very high load, but softening of the tissue matrix also decreased contractile strain. Consistent with these E4 results, softening of E6 hearts likewise impeded beating (Fig. 2D). A mathematical theory for striation [16] provides a basis for modeling contractile function with the equation:

$$Striation \sim \left[E/(E_m+E)^2 \right]^n \quad \text{(Eqn. 1)}$$

that fits experiments (Fig. 2C, dashed line; Supplement Box 1). The optimal stiffness for heart contraction is clearly the stiffness of native heart.

The speed of the contraction wave in each heart region increases monotonically with tissue stiffness, except for the most extreme rigidity (Fig. 2E). The linearity of wave speed can be predicted from a viscoelastic model of active media (Supplement Box 2). For the rigidified heart, beating was still evident, but the contraction wave did not propagate past the pacemaker region in the atrium (Fig. S2I). Softening treatments also decreased the probability of contractions propagating out of the atrium.

E4 and stem cell derived cardiomyocytes are highly sensitive to matrix elasticity

To assess whether variations in matrix elasticity affect E4-cardiomyocyte adhesion and beating, isolated cells and their properties were studied as sparse cultures on collagen-I

coated polyacrylamide gels of varied stiffness (Fig. 3A). Most of the cultured cells beat at 0.5-1.5 Hz, similar to the heart, indicating high viability as well as sustained adhesion. Relaxed morphologies were measured after 24 hr in culture and showed that substrates stiffer than E4 heart tissue promote spreading and elongation (Fig. S3A), as is common with other mesenchymal cell types (e.g. [12]). Cells on matrices of stiffness similar to that of the tissue of origin (∼1-2 kPa) were relatively round and unspread compared to the maximum achievable elongation and spreading. Nonetheless, contractile deformation of an E4 cardiomyocyte and its local matrix proves optimal at the matrix elasticity of native E4 tissue (Fig. 3B). In vitro contractions were measured in terms of both 2D strains using cell edge displacements and changes in aspect ratio.

Cardiomyocytes derived from embryonic stem cells (ESC-CM), induced pluripotent stem cells (iPS-CM) or directly transdifferentiated cells hold great potential for regenerative therapies [17], and human ESC-CM and iPS-CM displace soft matrix more than stiffer matrix [18]. Here, ESC-CM on soft, intermediate and stiff substrates that match immature (1 kPa), mature (11 kPa), and diseased (34 kPa) myocardium express at day-4 in culture similar levels of sarcomeric proteins but myofibril organization is visibly optimal for intermediate stiffness and contracting edge-velocities decrease with substrate stiffness (Fig. S3B-E). On soft substrates in day-6 cultures, myofibrils decrease and beating stops, while ESC-CM on the intermediate and stiff substrates bifurcated into either fast or slow contracting cell populations. Cardiogenesis is thus generally sensitive to matrix mechanics.

Optimal striation depends on Myosin-II contractile activity

Organization of the actomyosin cytoskeleton into sarcomeres and myofibrils within striated muscle cells is a well-established determinant of contractile activity [6, 8, 9], but in living zebrafish, fluorescence recovery after photobleaching shows striation proteins are mobile on timescales of 1-10 min [19]. Cardiomyocytes treated with the myosin-II ATPase inhibitor blebbistatin do not beat even though calcium transients are unaffected [20], and cells beat again within seconds after drug washout [21]. This is far quicker than contractility responses to heart matrix alterations in the 0.5-2 hr treatments here. To assess a role for myosin-II activity and contractile forces in striation as assumed in the modeling here [16] (Supplement Box 1), E7 cells with abundant striation were grown on gels optimal for striation [6], pulsed for 30 min with latrunculin to disassemble myofibrils, and then blebbistatin was added to half of the cultures (Fig. 3C,D). In the absence of blebbistatin, both premyofibrils and mature myofibrils recovered over a few hours from the induced disassembly, and most cells were filled with striations after 24 hr (Fig. 3D,E), whereas sustained blebbistatin suppressed striation, consistent with striation requiring active myosin-II.

Myofibril order depends on matrix elasticity *in vivo* and *in vitro*

With E4 hearts, we sought to quantify any possible striation differences with and without matrix alterations. Sarcomeric α-actinin-2 is a key crosslinker of 'z-discs' that is seen in mature myofibrils within embryos and also in shorter period premyofibrils using deconvolution microscopy [22]. In our confocal imaging, we measured sarcomere spacing lateral 'breadth' of z-discs along in-plane sarcomeres as a key metric of registry (Fig. 4A-inset). Whereas striation spacing peaked at 1.8 μm and appeared unaffected by ∼50%

softening of the E4 heart, the z-disc breadth was reduced relative to untreated control (Fig. 4B). This decreased registry of myofibrils shortly after softening of the matrix indicates a decreased coupling of sarcomeres and is consistent with the striation model [16], highlighting a molecular-scale mechanism for decreased contraction against decreased extracellular load.

Isolated cardiomyocytes beating on gels (Fig. 4C) show striation spacing of ~1 μm for premyofibrils, which conforms to expectations [19], and also the typical ~1.9 μm spacing of myofibrils (Fig.4D) evident in intact heart. Striation spacing shows no variation with matrix, but the abundance of myofibrils relative to premyofibrils is maximized on matrices of elasticity 2-10 kPa (Fig. 4E). This is consistent with myofibril assembly from premyofibrils [19]. The z-disc breadth of myofibrils also exhibited a broad and significant ($p < 0.05$) maximum (at ~2 μm breadth) within a similar range of matrix elasticities that promote myofibril formation (Fig. 4F). The premyobrils exhibited a somewhat narrower (~1.5 μm) z-disc breadth that at least decreased on the stiffest substrates. Myofibril structural trends in response to substrate stiffness in culture are thus consistent with intact E4 heart and suggest a common mechanism of stiffness-dependent registration.

Z-disc breadth results for both mature myofibrils and premyofibrils (Fig. 4F) were also fit by Eqn. 1 with respective E_m = 4.2±0.6 and 1.7±0.3 kPa (n = 0.24 ±0.1). Differences in E_m suggest myofibril organization favors a stiffer matrix or higher load. However, z-disc breadth also likely underestimates registration order within a cell, as it only includes immediately adjacent and perfectly registered striated fibers. Indeed, z-disc breadth trends for myofibrils and premyofibrils in isolated cells are broader than in simulation [16] but still consistent with trends for intact heart (Fig. 4B,F). What emerges systematically from fitting to Eq. 1 is that n increases with length scale: the smallest n is determined for z-disc breadth in culture and the largest n is found for strain in the intact heart. High cell density, 3D cell-matrix coupling, and cell-cell signaling in tissue (including calcium excitation waves) could all provide a basis for the enhanced sensitivity to matrix E of tissue.

Protein interactions that govern molecular mobility are force sensitive in living cardiomyocytes and vary with matrix elasticity [6]. An optimum stiffness for striation is thus understandable: while contractile activity 'massages' registration (Fig. 3E, 4) and these forces increase with matrix stiffness [1], high forces on stiff matrix tend to break bonds [6]. Myofibrils thereby mis-register if the load is either too low or high, which largely explains why *parallel and optimal* increases in actomyosin proteins and collagens (Fig. 1) must be coordinated in the tissue development program. Invading and proliferating fibroblasts make and remodel the matrix that stimulates cardiomyocyte proliferation [23] with increased expression of specialized contractile proteins (α-actinin-2, cardiac myosin-II in Fig. 1D,E), and so it is sensible that this program requires matrix engagement by integrins [23] and extends to mechanosensitive, adhesion complex proteins such as talin [24] that also increase (Fig. 1D). Moreover, since collagen synthesis and organization by fibroblasts is regulated by strain (as reviewed in [25]), heart matrix is likely to be optimized by the optimal stiffness for cardiomyocyte striation and contraction (Fig. 2-4). The fact that the optimum shifts in development from 1-2 kPa at E4 and at E7 toward the stiffness of adult heart (eg. Fig. 1C, 3E inset) [6, 8, 9] is also consistent with initial observations that hearts which were stiffened

and stop beating are found to re-start their beating ten hours later. Lastly, Excitation-Contraction Coupling (ECC) in muscle physiology is well-established [26], but the broad effects of matrix stiffness on individual cells and structures even in sparse culture preclude the confounding impacts of cell-cell electrical communication and suggest that Excitation-Contraction-*Matrix* Coupling (EC*M*C) is required to truly understand muscle.

Experimental Procedures

Heart isolation, enzyme treatments, micropipette analyses, tissue strain analyses, mass spectrometry proteomics, cell isolation, and the standard techniques are described in detail in Supplemental Methods.

Supplementary Material

Refer to Web version on PubMed Central for supplementary material.

Acknowledgments

References

1. Gonzalez-Rodriguez D, Guevorkian K, Douezan S, Brochard-Wyart F. Soft matter models of developing tissues and tumors. Science. 2012; 338(6109):910–917. [PubMed: 23161991]

2. Swift J, Ivanovska I, Buxboim A, Harada T, Dingal P, Pinter J, Pajerowski J, Spinler K, Shin J, Tewari M, Rehfeldt F, Speicher D, Discher D. Nuclear Lamin-A scales with tissue stiffness and enhances matrix-directed differentiation. Science. 2013; 341(6149)

3. Khetan S, Guvendiren M, Legant W, Cohen D, Chen C, Burdick J. Degradation-mediated cellular traction directs stem cell fate in covalently crosslinked three-dimensional hydrogels. Nature Materials. 2013

4. Chien K, Domian I, Parker K. Cardiogenesis and the complex biology of regenerative cardiovascular medicine. Science. 2008; 322(5907):1494–1497. [PubMed: 19056974]

5. Butcher JT, McQuinn TC, Sedmera D, Turner D, Markwald RR. Transitions in early embryonic atrioventricular valvular function correspond with changes in cushion biomechanics that are predictable by tissue composition. Integrative Physiology. 2007; 100:1503–1511.

6. Engler A, Carag-Krieger C, Johnson C, Raab M, Tang H, Spelcher D, Sanger J, Sanger J, Discher D. Embryonic cardiomyocytes beat best on a matrix with heart-like elasticity: scar-like rigidity inhibits beating. Journal of Cell Science. 2008; 10(24):3794–3802. [PubMed: 18957515]

7. Hersch N, Wolters B, Dreissen G, Springer R, Kirchgebner N, Merkel R, Hoffmann B. The constant beat: cardiomyocytes adapt their forces by equal contraction upon environmental stiffening. Biology Open. 2013; 2(3):351–361. [PubMed: 23519595]

8. Jacot J, McCulloch A, Omens J. Substrate Stiffness affects the functional maturation of neonatal rat ventricular myocytes. Biophysical Journal. 2008; 95:3479–3487. [PubMed: 18586852]

9. Rodriguez A, Han S, Regnier M, Sniadecki N. Substrate stiffness increases twitch power of neonatal cardiomyocytes in correlation with changes in myofibril structure and intracellular calcium. Biophysical Journal. 2011; 101(10):2455–2464. [PubMed: 22098744]

10. McCain M, Lee H, Aratyn-Schaus Y, Kleber A, Parker K. Cooperative coupling of cell-matrix and cell-cell adhesions in cardiac muscle. PNAS. 2012; 302(2):H445–H450.

11. Ulbricht A, Epplei F, Tapia V, van der Ven P, Hampe N, Hersch N, Vakeel P, stadel D, Haas A, Saftig P, Behrends C, Furst D, Volkmer R, Hoffmann B, Kolanus W, Hohfeld J. Cellular

mechanotransduction relies on tension-induced and chaperone-assisted autophagy. Current Biology. 2013; 23:430–435. [PubMed: 23434281]

12. Engler A, Sen S, Sweentey H, Discher D. Matrix elasticity directs stem cell lineage specification. Cell. 2006; 126(4):677–689. [PubMed: 16923388]

13. Theret D, Levesque M, Sato M, Nerem R, Wheeler L. The application of a homogeneous half-space model in the analysis of endothelial cell micropipette measurements. Journal of Biomechanical Engineering. 1988; 110:190–199. [PubMed: 3172738]

14. Georges P, Miller W, Meaney D, Sawyer E, Janmey P. Matrices with compliance comparable to that of brain tissue select neuronal over glial growth in mixed cortical cultures. Biophysical Journal. 2006; 90(8):3012–3018. [PubMed: 16461391]

15. Zamir AE, Srinivasan V, Perucchio R, Taber LA. Mechanical Asymmetry in the Embryonic Chick Heart During Looping. Annals of Biomedical Engineering. 2003; 31:1327–1336. [PubMed: 14758923]

16. Friedrich BM, Fischer-Friedrich E, Gov NS, Safran SA. Sarcomeric pattern formation by actin clustercoalescence. PLoS Computational Biology. 2012; 8(6):e1002544. [PubMed: 22685394]

17. Laflamme M, Murry C. Regenerating the heart. Nature Biotechnology. 2005; 23(7):845–846.

18. Hazeltine L, Simmons C, Salick M, Lian X, Badur M, Han W, Delgado S, Wakatsuki T, Crone W, Pruitt B, Palecek S. Effects of substrate mechanics on contractility of cardiomyocytes generated from human pluripotent stem cells. International Journal of Cell Ciology. 2012; 2012

19. Sanger JW, Wang J, Holloway B, Du A, Sanger JM. Myofibrillogenesis in Skeletal Muscle Cells in Zebrafish. Cell Motility and Cytoskeleton. 2009; 66(8):556–566.

20. Shwarek-Maruszewska A, Hotulainen P, Mattila P, Lappalainen P. Contractility dependent actin dynamics in cardiomyocyte sarcomeres. Journal of Cell Science. 2009; 112:2119–2126.

21. Farman GP, Tachampa K, Mateja R, Cazorla O, Lacampagne A, de Tombe PP. Blebbistatin: use as inhibitor of muscle contraction. Pflugers Archiv. 2008; 455(6):995–1005. [PubMed: 17994251]

22. Du A, Sanger J, Sanger J. Cardiac myofibrillogenesis inside intact embryonic heart. Developmental Biology. 2008; 318(2):236–246. [PubMed: 18455713]

23. Ieda M, Tsuchihashi T, Ivey K, Ross R, Hong T, Shaw R, Srivastava D. Cardiac Fibroblasts Regulate Myocardial Proliferation through B1 Integrin Signaling. Developmental Cell. 2009; 16:233–244. [PubMed: 19217425]

24. del Rio A, Perez-Jimenez R, Liu R, Roca-Cusachs P, Fernandez J, Sheetz M. Stretching single talin rod molecules activate vinculin binding. Science. 2009; 323(5914):638–641. [PubMed: 19179532]

25. Baudino T, Carver W, Giles W, Borg T. Cardiac fibroblasts: friend of foe? American Journal of Physiology Heart and Circulatory Physiology. 2006; 291:H1015–H1026. [PubMed: 16617141]

26. Bers, D. Excitation-Contraction Coupling and Cardiac Contraction Force. 2nd. Boston, MA: Kluwer Academic Publishers; 2001.

27. Khalilian M, Navidbakhsh M, Valojerdi M, Chizari M, Yazdi P. Estimating Young's modulus of zona pellucida by micropipette aspiration in combination with theoretical models. J R Soc Interface. 2010; 7:687–694. [PubMed: 19828504]

28. Bajaj P, Tang X, Saif T, Bashir R. Stiffness of the substrate influences the phenotype of embryonic chicken cardiac myocytes. J Biomed Mater Res Part A. 2010; 95(4):1261–1269.

29. Bhana B, Iyer R, Chen W, Zhao R, Sider K, Likhitpanichkul M, Simmons C, Radisic M. Influence of substrate stiffness on the phenotype of heart cells. Biotechnology and Bioengineering. 2009; 105(6):2151–2162.

Highlights

- Embryonic heart is stiffer than early embryo but softer than mature heart.

- Stiffening parallels expression of excitation-contraction proteins plus collagen-I.

- Stiffening or softening collagen in heart reveals optimal stiffness for beating.

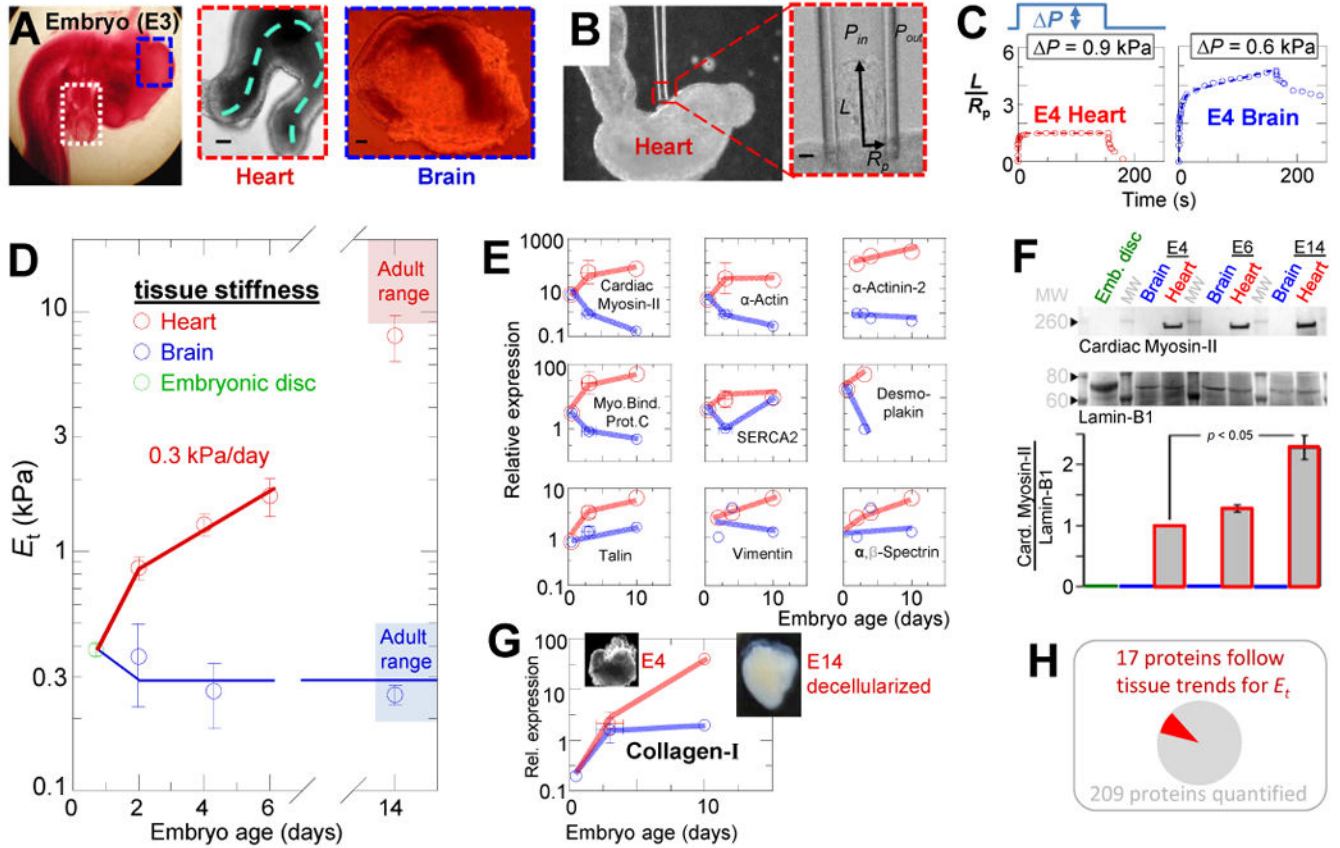- In culture, embryonic heart cells exhibit the same optimal stiffness.

Fig. 1. Mechanical development of heart and brain tissue parallels expression of abundant cell and matrix proteins

(**A**) E3 chick embryo with heart tube (white box) and midbrain (blue box) *in situ* and after isolation. The heart continues to beat *ex vivo*, with contraction and flow propagating along the dashed line. Scale = 100 μm. (**B**) Micropipette aspiration of an E3 heart tube in phase contrast microscopy. Scale = 10 μm. (**C**) Representative aspiration and relaxation curves for E4 heart and brain demonstrate the respective elastic and inelastic responses. (**D**) E_t for heart and brain tissue throughout embryonic development, starting with day-1 embryonic disk, then E2, E4, E6, and E14 heart and brain (n 3 measurements each). By the time beating starts, the heart is already 3-fold stiffer than early embryonic tissue and then stiffens at a rate of 0.3 kPa/day. Due to the thick epicardium of E6 hearts and older relative to the inner diameter of our micropipettes, measurements likely underestimate stiffness of the myocardium at those stages due to significant contribution of epicardium. Brain tissue does not stiffen during development and remains viscoelastic with a mean E_t = 0.3 kPa. (**E**) Quantitative mass spectrometry (MS) of cellular proteins extracted from intact embryonic disc (Hamburger-Hamilton stage 3-4), E2, E3, E4, and E10 heart and brain tissue reveals a small set of detected proteins with expression patterns similar to heart or brain mechanics: namely, a general increase in heart and relatively small increase in brain. Expression is relative to average in brain E2-E3 (n 3 MS measurements). (**F**) Immunoblot confirms that MS measurements of Cardiac Myosin-II expression increase in heart development. Samples are pooled from 3-4 embryos at each reported stage and were normalized to Lamin-B1 (n

3). (**G**) MS indicates that collagen-I expression increases during heart development, but not greatly during brain development. Inset images: 1% SDS-decellularized E4 and E14 hearts. The insoluble matrices retain the shape of the embryonic hearts, but while E14 matrix (with 80% of MS ion current being collagen-1) appears solid, the E4 matrix appears more reticulated and porous, consistent with relatively less mass. (**H**) Of the proteins identified by Mass-Spec (Table S1), a small subset had expression levels across tissues and development that paralleled mechanics. Error bars in all figures represent SEM.
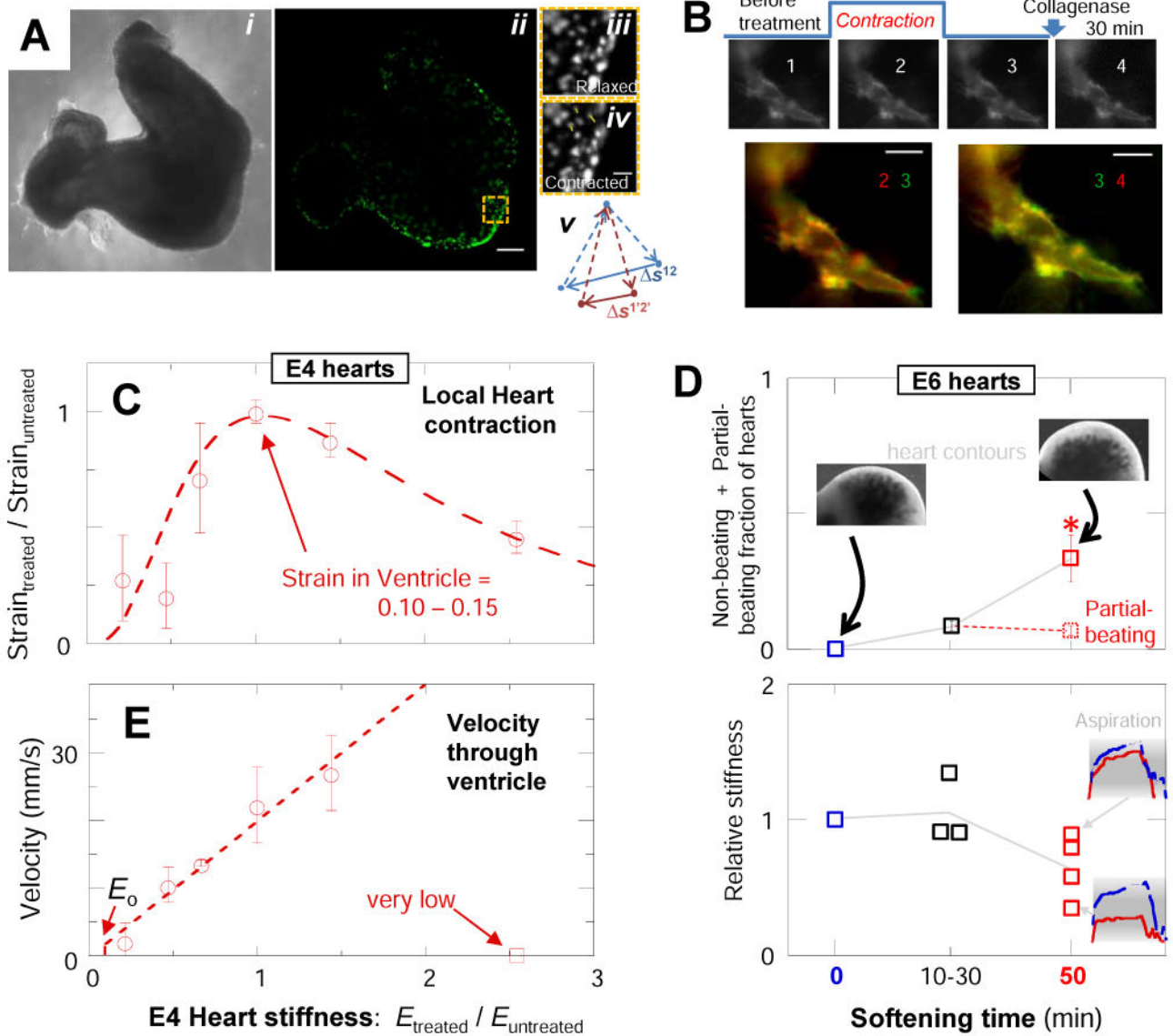
Fig. 2. Effect of extracellular matrix softening and stiffening on heart tube beating
(**A**) E4 heart imaged by (**i**) phase contrast or (**ii**) fluorescence after sparse transfection with GFP. Scale = 100 um. Three GFP-expressing cells used to calculate strain during beating are tracked from their relaxed (**iii**) to contracted positions (**iv**, scale = 20 μm). Strain is schematized in (**v**) per [28]. (**B**) SIRPA-GFP-expressing cell in transfected E4 heart tissue before and after softening. Overlays of SIRPA-GFP expressing cells over time help visualize cell conformational changes during contraction and softening treatments. Overlay of the same cell pre-treatment while relaxed (green) and contracted (red) (bottom-left) shows less overlap (yellow) than the relaxed cell before and after tissue softening; cells thus maintain morphology and adhesions during softening. (**C**) Tissue strain during beating of GFP-transfected softened and stiffened E4 heart normalized to that of untreated and the resulting relative strain averaged for atria, ventricles, and outflow tract: softened and stiffened tissues suppress contractions. Typical peak strains throughout the untreated heart tube were 10 ±

4%. The dashed curve is a fit to Eq. 1 with exponent $n = 4 \pm 1$ and $E_m = 1.6 \pm 0.2$ kPa. (**D**) E6 hearts treated progressively with collagenase stop beating or only beat partially. Beating is suppressed after 50 min softening treatment, relative to untreated or briefly (10-30 min) treated hearts ($p = 0.016$). Insets: representative aspiration-relaxation curves for mildly softened or considerably softened hearts. Red indicates untreated tissue and blue indicates treated tissue. (**E**) Velocity of the contraction wave through the ventricle vs normalized E_t. Wave-speeds in untreated ventricle, atria, and outflow tract of 22 ± 4 mm/s, 4 ± 2 mm/s and 2.8 ± 0.7 mm/s, respectively, are consistent with past work [29]. For the most extreme stiffening treatment, contraction does not propagate past the presumptive pacemaker. The velocity in the ventricle increases linearly with tissue stiffness. The dashed line is the theoretical prediction with a single adjustable parameter, namely the ratio of the stress threshold to the magnitude of the force dipole corresponding to a contracting cell. E_o indicates the theoretically predicted stiffness below which a contraction wave should not propagate. Error bars for all figures represent SEM (n   3 hearts).
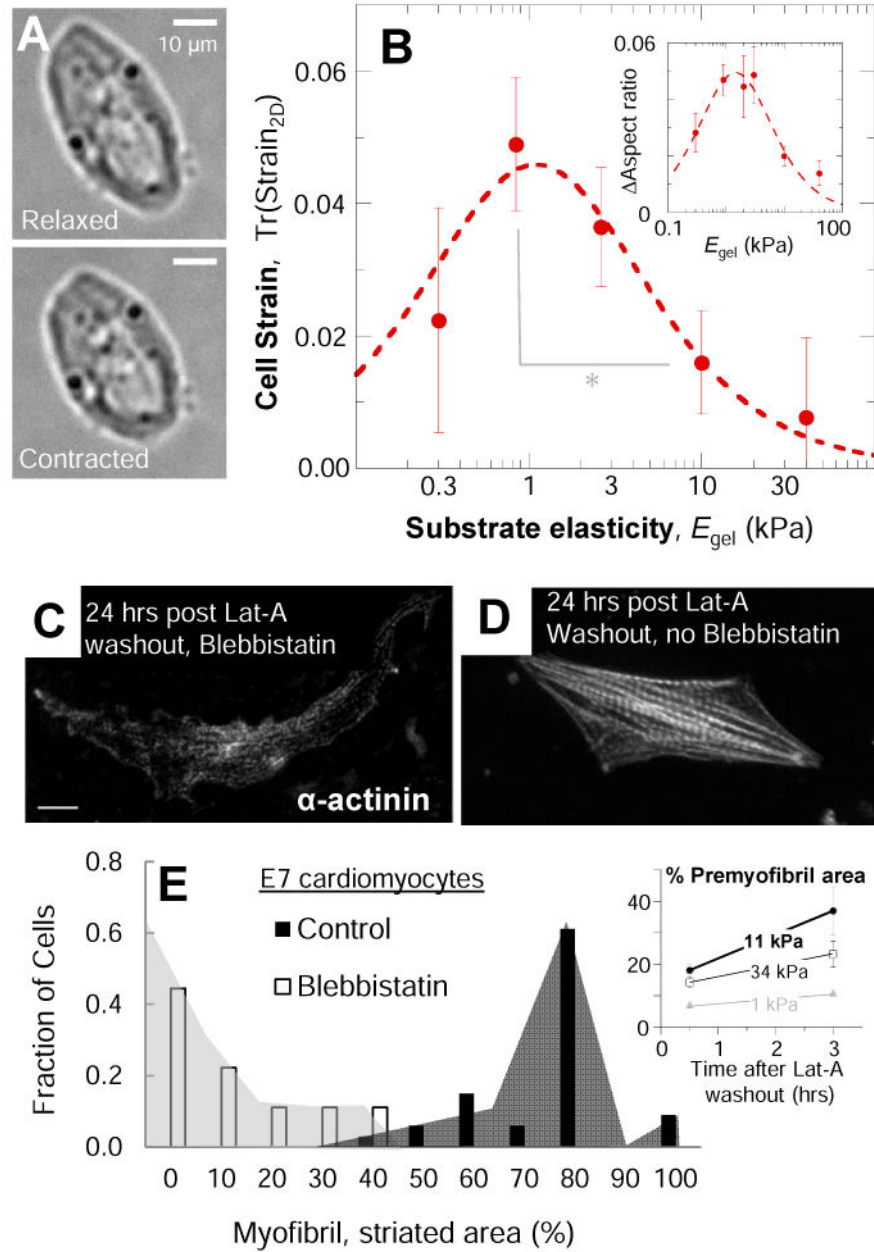
Fig. 3. Isolated cardiomyocytes are sensitive to matrix stiffness, with striation dependent on actomyosin work

(**A**) Cardiomyocytes were imaged beating in culture after 18-24 hr in culture. Morphologies in the relaxed and contractile states and contractile strains were measured for beating cells. (**B**) Edge-strain of cardiomyocytes cultured on PA gels of various stiffnesses, measured as the trace of the 2D strain-matrix of cell edge points during beating, as described in methods. In beating, cell and matrix strain is strongly modulated by substrate elasticity with an optimal E_{gel} similar to that of E4 heart and much lower than that measured for more mature cells ([6, 8]). Softer and stiffer substrates impede beating of cultured cells. The Lorentzian fit gives $E_m = 1.3 \pm 0.3$ kPa, consistent with the tissue elasticity of E4 hearts ($E_t = 1.3 \pm 0.4$ kPa in Fig. 1). (**C-D**) Representative image of E7 cardiomyocytes recovering from

latrunculin-A (Lat-A) treatment in the presence (**C**) or absence (**D**) of blebbistatin, which does not affect cell viability [12]. (**E**) Myofibril assembly was measured as the percentage of cell area covered by mature myofibrils (sarcomere spacing > 1.5 um). Inhibition of beating and actomyosin contractility by blebbistatin reduces the amount of new myofibrils formed following Lat-A washout and causes mature myofibrils to disassemble per (**C**). Inset shows that for these late embryo cardiomyocytes, the optimal elasticity for rapid recovery of striated pre-myofibrils is close to that of adult heart ($E_t \sim 10\text{-}15$ kPa). Error bars are SEM (n 3 cells). (*) $p < 0.05$.
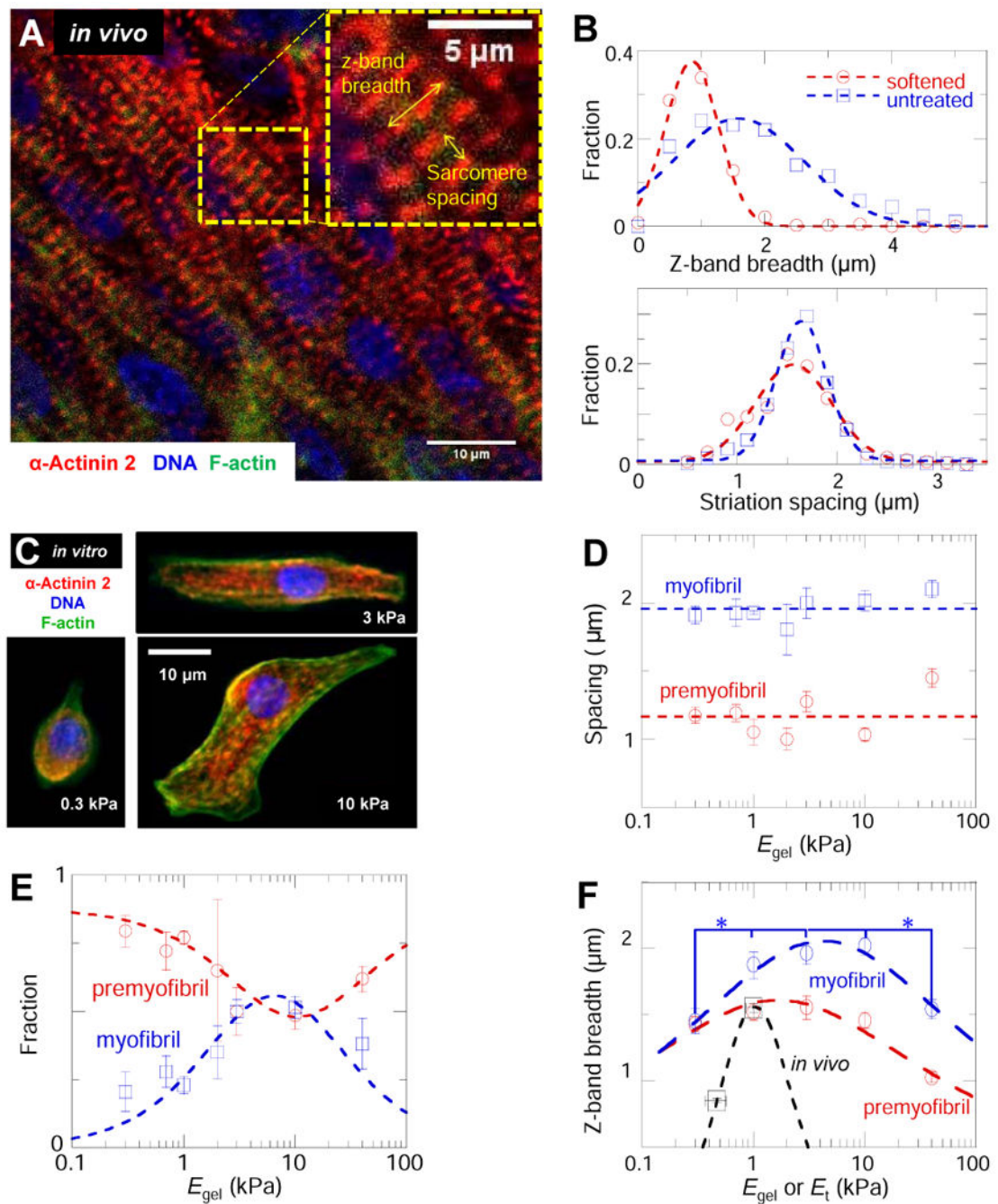
Fig. 4. Sarcomere breadth changes in softened heart and in isolated cardiomyocytes on compliant substrates

(**A**) Untreated and softened whole E4 hearts were immunostained for sarcomeric α-actinin-2, F-actin, and DNA and imaged by confocal microscopy. Sarcomere spacing and Z-disc breadth (inset) were measured to assess any structural changes. (**B**) Z-disc breadth is significantly decreased in the 47%-softened heart relative to untreated controls. The decreased registry of myofibrils suggests a decreased coupling between adjacent myofibrils during contraction. Sarcomere spacing is consistent with mature myofibril sarcomere

spacing and is not significantly different in the softened and untreated hearts. (**C**) E4 cardiomyocytes cultured on gels were stained in the same way as the whole hearts of figure A. Figure shows typical E4 cardiomyocytes on gels with stiffnesses of 0.3, 3.0 and 10 kPa. (**D**) Striation spacing was bimodal in distribution, indicating mature myofibrils (sarcomere spacing > 1.8 um) as well as pre-myofibrils (sarcomere spacing < 1.4 um). (**E**) Fraction of each type of striation per cell with myofibrils maximal on gels where pre-myofibrils are minimal. We fit the fraction of myofibrils with $f_m = f$ (Eq. 1), (blue dashed line) and pre-myofibrils using $f_p = 1 \& -f_m$ with $E_m = 9 \pm 2$ kPa. (**F**) Z-disc breadth for myofibrils and pre-myofibrils were maximized on substrates of intermediate stiffness. Fits to Eq. 1 yield $E_m = 1.7 \pm 0.3$ kPa for pre-myofibrils and $E_m = 4.2 \pm 0.6$ kPa for myofibrils. Error bars are SEM (n ≥ 3 hearts or cells).